Ocean Heat

Identification

1. Indicator Description

This indicator describes trends in the amount of heat stored in the world's oceans between 1955 and 2020. The amount of heat in the ocean, or ocean heat content, is an important indicator of climate change because the oceans ultimately absorb a large portion of the extra energy that greenhouse gases trap near the Earth's surface. Ocean heat content also plays an important role in the Earth's climate system because heat from ocean surface waters provides energy for storms and thereby influences weather patterns.

2. Revision History

April 2010:	Indicator published.
December 2012:	Updated indicator with data through 2011.
August 2013:	Updated indicator with data through 2012.
May 2014:	Updated indicator with data through 2013.
June 2015:	Updated indicator with data through 2014.
August 2016:	Updated indicator with data through 2015.
April 2021:	Updated indicator with data through 2020, added new IAP data source, updated MRI/JMA analysis version, and added Figure 2 to present measurements from a deeper portion of the water column.

Data Sources

3. Data Sources

This indicator is based on analyses conducted by four government organizations:

- Australia's Commonwealth Scientific and Industrial Research Organisation (CSIRO)
- The Japan Meteorological Agency's Meteorological Research Institute (MRI/JMA)
- The U.S. National Oceanic and Atmospheric Administration (NOAA)
- The Chinese Academy of Sciences' Institute of Atmospheric Physics (IAP)

NOAA, IAP, and MRI/JMA used data from the World Ocean Database (WOD) for their analyses. MRI/JMA also used data from two other data sets: the Global Temperature-Salinity Profile Program (GTSPP, which was used to fill gaps in the WOD since 1990) and the Argo Project. CSIRO used two data sets: ocean temperature profiles in the UK Met Office's ENACT/ENSEMBLES version 4 (EN4) database and data collected by thousands of Argo profiling floats. Information on Argo project can be found at: https://argo.ucsd.edu. Additionally, CSIRO included bias-corrected Argo data, as described in Barker et al. (2011), and bias-corrected expendable bathythermograph (XBT) data from Wijffels et al. (2008). NOAA also used data from the WOA in addition to the WOD.

4. Data Availability

EPA developed Figure 1 using trend data from several ongoing studies. Data and documentation from these studies can be found at the following links:

- CSIRO: www.cmar.csiro.au/sealevel/thermal_expansion_ocean_heat_timeseries.html. Select "GOHC_recons_version3.1_1950_2012_CLIM_sbca12tmosme_OBS_bcax_0700m.dat" to download data through 2012. See additional documentation in Domingues et al. (2008). Updated data through 2015 were provided by the author, Catia Domingues.
- IAP: http://159.226.119.60/cheng. Updated data through 2020 were provided by the author, Lijing Cheng, before being posted on this website. See additional documentation in Cheng et al. (2017).
- MRI/JMA: www.data.jma.go.jp/gmd/kaiyou/english/ohc/ohc_global_en.html. Select "Heat content anomaly time series."
- NOAA, 0–700 meters: www.nodc.noaa.gov/OC5/3M_HEAT_CONTENT. Under "Heat Content," select "Basin time series fields." Then, under "Yearly from 1955 to 2020," select the "0 - 700" file under "World." See additional documentation in Levitus et al. (2009).
- NOAA, 0–2,000 meters: www.nodc.noaa.gov/OC5/3M_HEAT_CONTENT. Under "Heat Content," select "Basin time series fields." Then, under "Pentadal from 1955 to 2020," select the "0 - 2000" file under "World." See additional documentation in Levitus et al. (2012).

The underlying data for this indicator come from a variety of sources. Some of these data sets are publicly available; others consist of samples gathered by the authors of the source papers, and these data might be more difficult to obtain online. WOA and WOD data and descriptions of data are available on NOAA's National Centers for Environmental Information (NCEI) website at: www.nodc.noaa.gov/OC5/3M_HEAT_CONTENT. The EN4 database is available at: www.metoffice.gov.uk/hadobs/en4.

Methodology

5. Data Collection

Figure 1 of this indicator reports on the amount of heat stored in the ocean from sea level to a depth of 700 meters, which accounts for approximately 17.5 percent of the total global ocean volume (calculation from Catia Domingues, CSIRO). Figure 2 reports on the amount of heat stored to a depth of 2,000 meters, which accounts for approximately 48.5 percent of the total global ocean volume (calculation from Catia Domingues, CSIRO). Each of the studies used to develop this indicator uses several ocean temperature profile data sets to calculate an ocean heat content trend line.

Several different devices are used to sample temperature profiles in the ocean. Primary methods used to collect data for this indicator include XBT; mechanical bathythermographs (MBT); Argo profiling floats; reversing thermometers; and conductivity, temperature, and depth sensors (CTD). These instruments produce temperature profile measurements of the ocean water column by recording data on temperature and depth. The exact methods used to record temperature and depth vary. For instance, XBTs use a fall rate equation to determine depth, whereas other devices measure depth directly.

Each of the studies used to develop this indicator relies on different combinations of devices; for example, the CSIRO analysis excludes MBT data. More information on the main studies and their respective methods can be found at:

- CSIRO: Domingues et al. (2008) and: www.cmar.csiro.au/sealevel/thermal_expansion_ocean_heat_timeseries.html.
- IAP: Cheng et al. (2017) and: http://159.226.119.60/cheng.
- MRI/JMA: Ishii et al. (2017).
- NOAA, 0–700 meters: Levitus et al. (2009) and: www.nodc.noaa.gov/OC5/3M_HEAT_CONTENT.
- NOAA, 0–2,000 meters: Levitus et al. (2012) and: www.nodc.noaa.gov/OC5/3M_HEAT_CONTENT.

Studies that measure ocean temperature profiles are generally designed using in situ oceanographic observations and analyzed over a defined and spatially uniform grid (Ishii and Kimoto, 2009). For instance, the WOA data set consists of in situ measurements of climatological fields, including temperature, measured in a 1-degree grid. Sampling procedures for WOD and WOA data are provided by NOAA's NCEI at: www.nodc.noaa.gov/OC5/indprod.html. More information on the WOA sample design in particular can be found at: www.nodc.noaa.gov/OC5/WOA05/pr_woa05.html.

At the time of this indicator's last update, data from CSIRO were available through 2015, data from IAP were available through 2020, MRI/JMA data were available through 2020, and NOAA data were available through 2020. NOAA's 0–2,000 meter data are plotted from 1957 through 2018 because each annual value is derived from a pentadal average, the earliest of which covered 1955–1959 and the most recent of which covered 2016–2020.

6. Indicator Derivation

While details of data analysis are particular to the individual study, in general, temperature profile data were averaged monthly at specific depths within rectangular grid cells. In some cases, interpolation techniques were used to fill gaps where observational spatial coverage was sparse. Additional steps were taken to correct for known biases in XBT data. Finally, temperature observations were used to calculate ocean heat content through various conversions.

Barker et al. (2011) describe instrument biases and procedures for correcting for these biases. For more information about interpolation and other analytical steps, see Cheng et al. (2017), Ishii et al. (2017), Domingues et al. (2008), Levitus et al. (2009), Levitus et al. (2012), and references therein.

Each study used a different long-term average as a baseline. To allow more consistent comparison, EPA adjusted each curve such that its 1971–2000 average would be set at zero. Choosing a different baseline period would not change the shape of the data over time. Although some of the studies had pre-1955 data, Figure 1 begins at 1955 for consistency. The current CSIRO data series is based on updates to the original data set provided in Domingues et al. (2008) and plotted with a start date of 1960. The updated data set excludes 1955–1959: the authors (Domingues et al.) have expressed diminished confidence in their data set for this period because there are fewer ocean observations in the early part of the record. The data set also uses a three-year running mean to smooth the data.

NOAA calculated its 0–2,000 meter data set using pentadal (five-year) averages due to the relative paucity of underlying data points in the deep ocean, particularly for the early portion of the time series. NOAA published annual values that are derived from this pentadal data product.

Indicator Development

EPA has periodically enhanced this indicator to reflect ongoing improvements in data sources and methods of estimating global ocean heat content. Prior to 2018, this indicator focused on data from three sources—CSIRO, MRI/JMA, and NOAA—covering the top 700 meters of the world oceans. With the publication of enhanced methods for reconstructing deeper ocean heat trends in Cheng et al. (2017), EPA was able to add a new source (IAP) to Figure 1 and was also able to create Figure 2 with data for the top 2,000 meters of the ocean. Figure 2 also includes improved estimates for the top 2,000 meters from NOAA and MRI/JMA.

For reference, Figure TD-1 shows the relative changes in heat content of the 0–700 meter and 700–2,000 meter layers of the world's oceans, based on the IAP analysis (updated from Cheng et al., 2017). The total height of the stack represents the total change across both of these segments of the water column. Like Figures 1 and 2, Figure TD-1 is normalized to the 1971–2000 mean.

Figure TD-1. Relative Contributions to Changes in Ocean Heat Content in the IAP Data Set, by Depth, 1955–2020

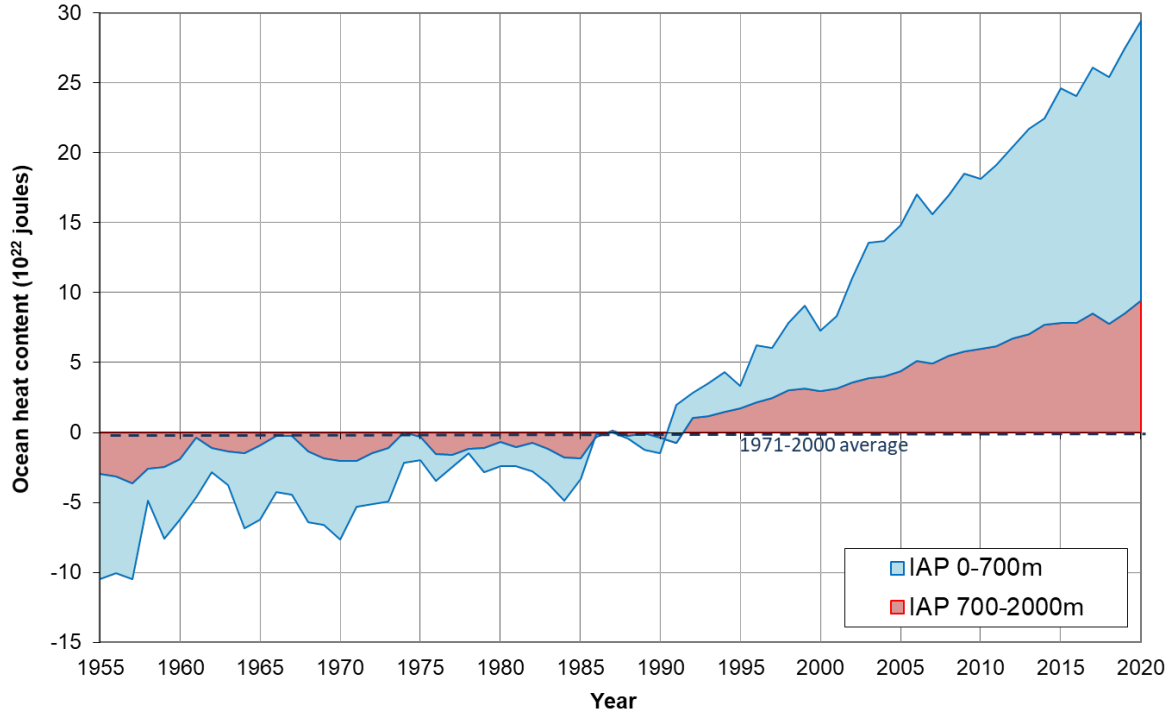

Data source: IAP 2021 update to data originally published in Cheng et al. (2017).

7. Quality Assurance and Quality Control

Data collection and archival steps included quality assurance/quality control (QA/QC) procedures. For example, QA/QC measures for the WOD are available in documents at:

www.nodc.noaa.gov/OC5/WOD/docwod.html. Each of the data collection techniques involves different QA/QC measures. For example, a summary of studies concerning QA/QC of XBT data is available from NCEI at: www.nodc.noaa.gov/OC5/XBT_BIAS/xbt_bibliography.html. The same site also provides additional information about QA/QC of ocean heat data made available by NCEI.

All of the analyses performed for this indicator included additional QA/QC steps. In each of the main studies used in this indicator, the authors carefully describe QA/QC methods, or provide the relevant references.

Analysis

8. Comparability Over Time and Space

Analysis of raw data is complicated because data come from a variety of observational methods, and each observational method requires certain corrections to be made. For example, systematic biases in XBT depth measurements have recently been identified. These biases were shown to lead to erroneous estimates of ocean heat content through time. Each of the main studies used in this indicator corrects for these XBT biases. Correction methods are slightly different among studies and are described in detail in each respective paper. More information on newly identified biases associated with XBT can be found in Barker et al. (2011).

This indicator presents multiple independently derived trend lines to compare different estimates of ocean heat content over time. Each estimate is based on analytical methods that have been applied consistently over time and space. General agreement among trend lines, despite some year-to-year variability, indicates a robust trend.

9. Data Limitations

Factors that may impact the confidence, application, or conclusions drawn from this indicator are as follows:

1. Data must be carefully reconstructed and filtered for biases because of different data collection techniques and uneven sampling over time and space. Various methods of correcting the data have led to slightly different versions of the ocean heat trend line.

2. In addition to differences among methods, some biases may be inherent in certain methods. The older MBT and XBT technologies have the highest uncertainty associated with measurements.

3. Limitations of data collection over time and especially over space affect the accuracy of observations. In some cases, interpolation procedures were used to complete data sets that were spatially sparse.

10. Sources of Uncertainty

Uncertainty measurements can be made by the organizations responsible for data collection, and they can also be made during subsequent analysis. One example of uncertainty measurements performed by an agency is available for the WOA at: www.nodc.noaa.gov/OC5/indprod.html.

Error estimates associated with each of the curves in Figure 1 are discussed in Cheng et al. (2017), Domingues et al. (2008), Ishii et al. (2017), Hirahara et al. (2014), and Levitus et al. (2009). Error estimates for Figure 2 are discussed in Cheng et al. (2017), Levitus et al. (2012), Ishii et al. (2017), and Hirahara et al. (2014).

Each of the data files listed in Section 4 includes some type of error or uncertainty around each data point. Figures TD-2, TD-3, TD-4, and TD-5 show these error or uncertainty values. To be true to each of the original sources, these figures show the values as they were provided, and they use the corresponding nomenclature as reported by the organization that published the data. The shaded error or uncertainty bands in these four figures represent different statistical properties, so they are not directly comparable to each other. Figure TD-3 shows monthly values; it shows the 700–2,000 meter segment of the water column (not 0–2,000 meters) because that is how IAP reported the original data. No attempt was made to transform these numbers into annual error estimates or to calculate combined error values for the sum of the 0–700 meter and 700–2,000 meter sections.

Figure TD-2. Ocean Heat Content in the Top 700 Meters from the CSIRO Data Set, 1960–2015, with One Standard Deviation

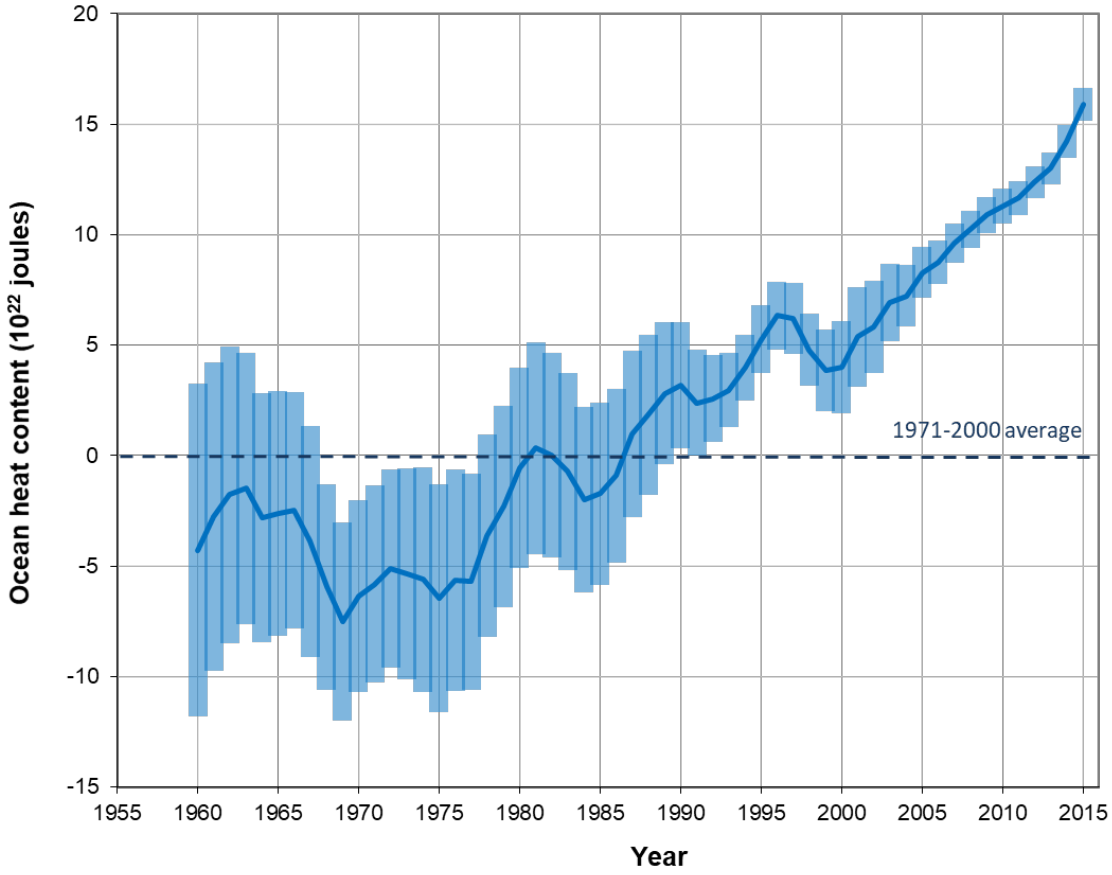

Data source: CSIRO 2016 update to data originally published in Domingues et al. (2008).

Figure TD-3. Ocean Heat Content for 0–700 Meters and 700–2,000 Meters from the Monthly IAP Data Sets, 1955–2017, with 95 Percent Confidence Intervals

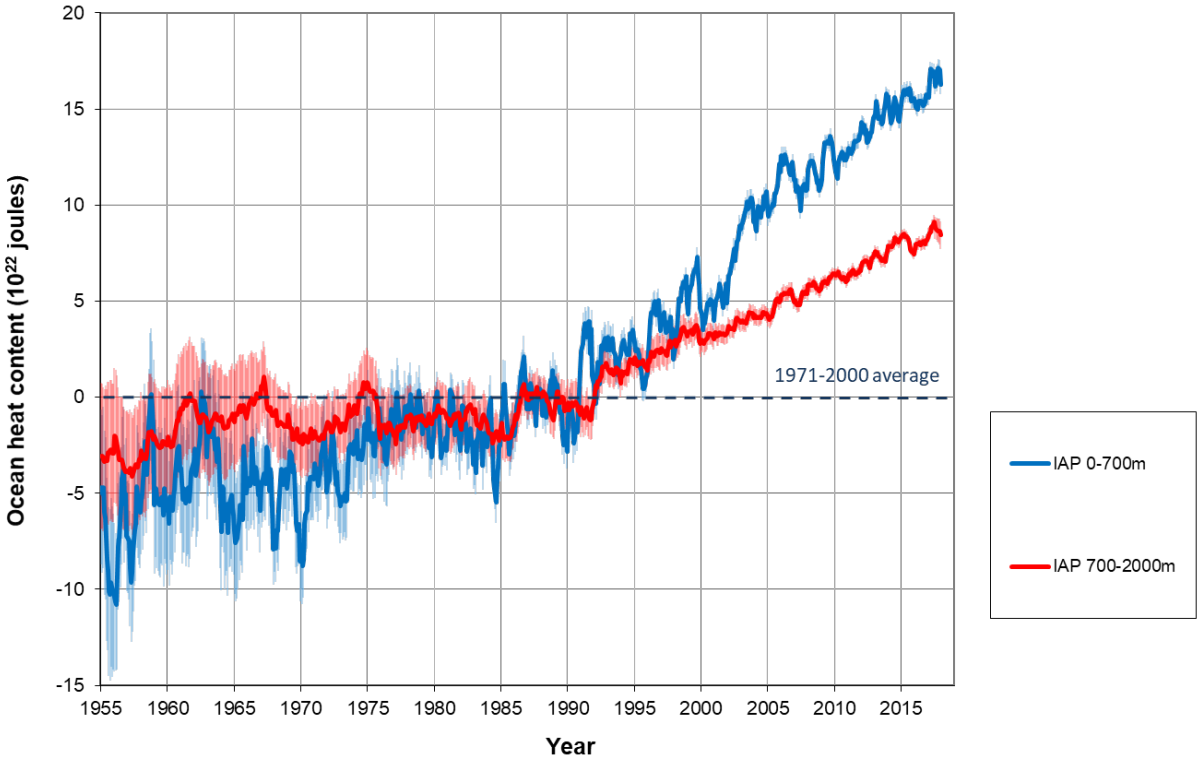

Data source: Cheng et al. (2017).

Figure TD-4. Ocean Heat Content for the Top 2,000 Meters from the MRI/JMA Data Set, 1955–2020, with 95 Percent Confidence Intervals

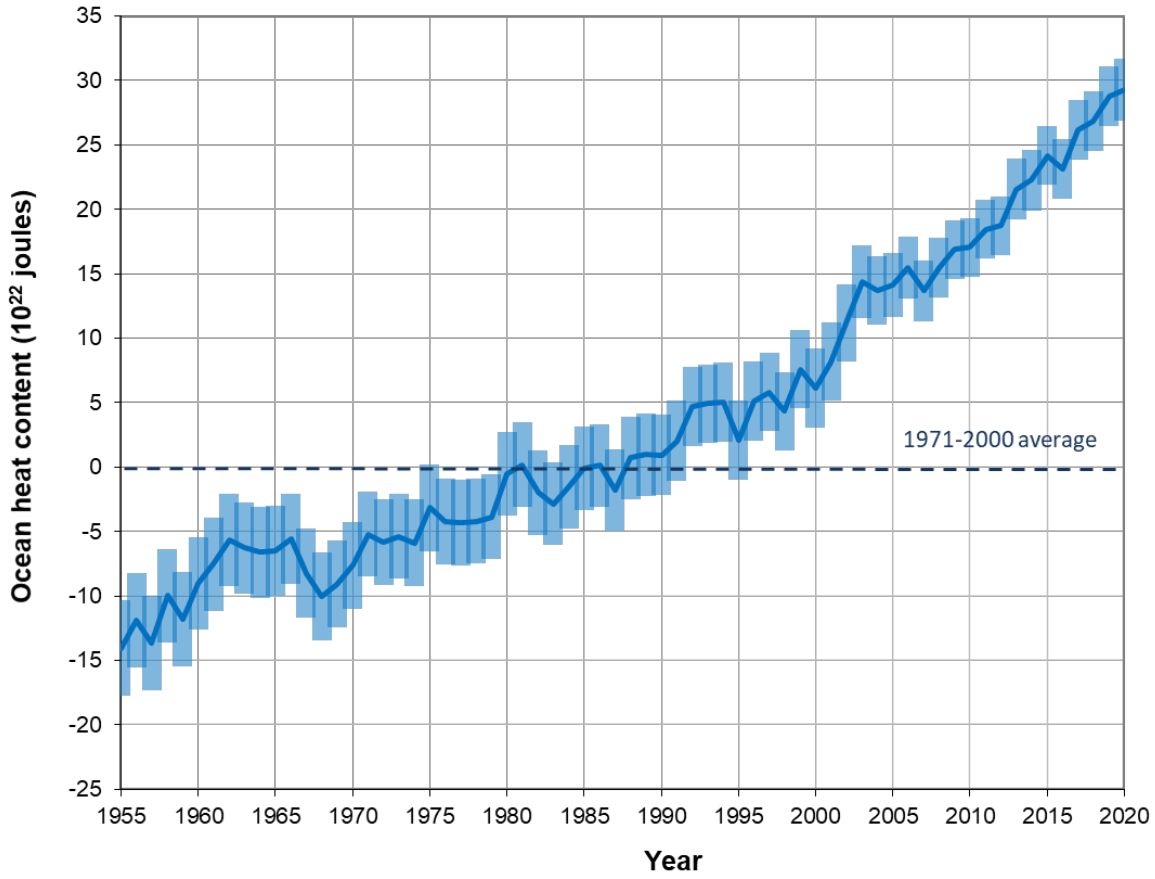

Data source: MRI/JMA data portal: www.data.jma.go.jp/gmd/kaiyou/english/ohc/ohc_global_en.html.

Figure TD-5. Ocean Heat Content in the Top 700 Meters and the Top 2,000 Meters in the NOAA Data Sets, 1955–2020, with Standard Errors

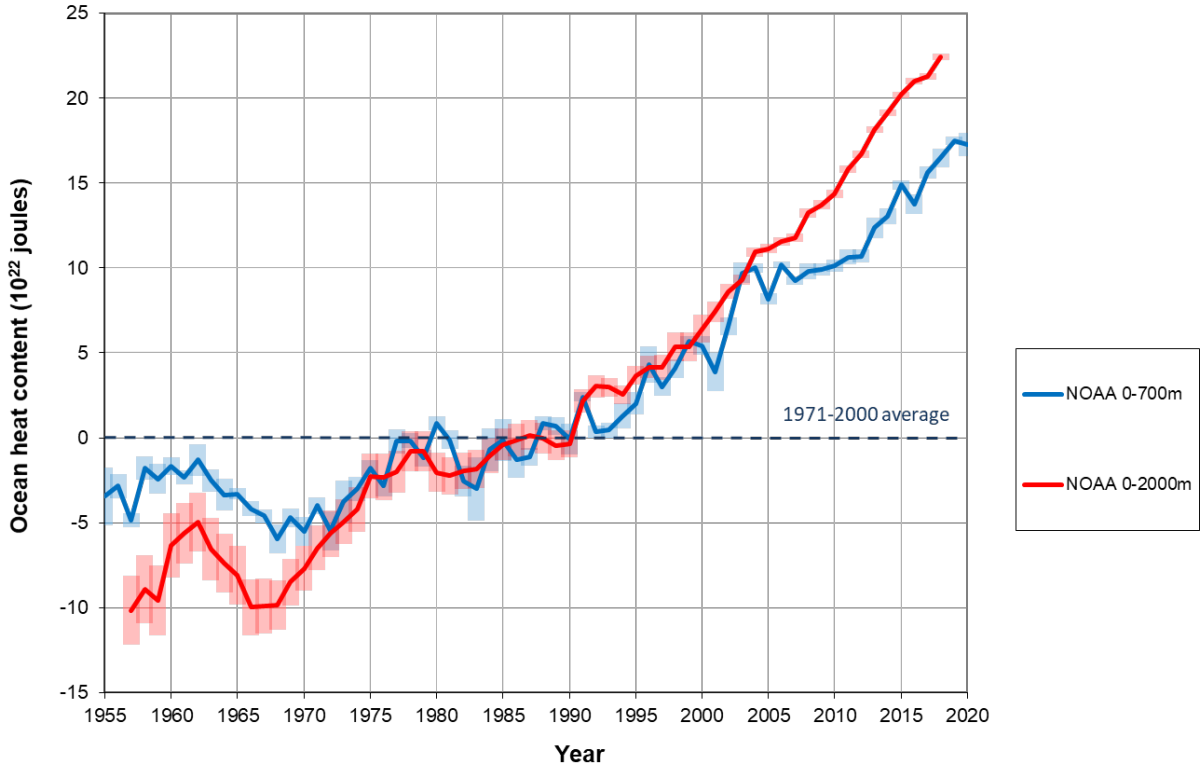

Data source: NOAA data portal: www.nodc.noaa.gov/OC5/3M_HEAT_CONTENT.

11. Sources of Variability

Weather patterns, seasonal changes, multiyear climate oscillations, and many other factors could lead to day-to-day and year-to-year variability in ocean temperature measurements at a given location. This indicator addresses some of these forms of variability by aggregating data over time and space to calculate annual values for global ocean heat content. The overall increase in ocean heat over time (as shown by all of the analyses) far exceeds the range of interannual variability in ocean heat estimates.

12. Statistical/Trend Analysis

Cheng et al. (2017), Domingues et al. (2008), Levitus et al. (2009), and Levitus et al. (2012) have all calculated linear trends and corresponding error values for their respective ocean heat time series. Ishii et al. (2017) calculated trends using the leading empirical orthogonal function interpolated to a 1-degree grid; see Hirahara et al. (2014) for more details. Exact time frames and slopes vary among the publications, but they all reveal a statistically significant upward trend (i.e., increasing ocean heat over time).

References

Barker, P.M., J.R. Dunn, C.M. Domingues, and S.E. Wijffels. 2011. Pressure sensor drifts in Argo and their impacts. J. Atmos. Oceanic Tech. 28:1036–1049.

Cheng, L., K.E. Trenberth, J. Fasullo, T. Boyer, J. Abraham, and J. Zhu. 2017. Improved estimates of ocean heat content from 1960 to 2015. Science Advances 3(3):e1601545.

Domingues, C.M., J.A. Church, N.J. White, P.J. Gleckler, S.E. Wijffels, P.M. Barker, and J.R. Dunn. 2008. Improved estimates of upper-ocean warming and multi-decadal sea-level rise. Nature 453:1090–1093.

Hirahara, S., M. Ishii, and Y. Fukuda. 2014. Centennial-scale sea surface temperature analysis and its uncertainty. J. Climate 27(1):57–75.

Ishii, M., and M. Kimoto. 2009. Reevaluation of historical ocean heat content variations with time-varying XBT and MBT depth bias corrections. J. Oceanogr. 65:287–299.

Ishii, M., Y. Fukuda, H. Hirahara, S. Yasui, T. Suzuki, and K. Sato. 2017. Accuracy of global upper ocean heat content estimation expected from present observational data sets. SOLA 13:163–167. https://www.jstage.jst.go.jp/article/sola/13/0/13_2017-030/_article. doi:10.2151/sola.2017-030

Levitus, S., J.I. Antonov, T.P. Boyer, R.A. Locarnini, H.E. Garcia, and A.V. Mishonov. 2009. Global ocean heat content 1955–2008 in light of recently revealed instrumentation problems. Geophys. Res. Lett. 36:L07608.

Levitus, S., J.I. Antonov, T.P. Boyer, O.K. Baranova, H.E. Garcia, R.A. Locarnini, A.V. Mishonov, J.R. Reagan, D. Seidov, E.S. Yarosh, and M.M. Zweng. 2012. World ocean heat content and thermosteric sea level change (0–2000 m), 1955–2010. Geophys. Res. Lett. 39(10):L10603. doi:10.1029/2012GL051106

Wijffels, S.E., J. Willis, C.M. Domingues, P. Barker, N.J. White, A. Gronell, K. Ridgway, and J.A. Church. 2008. Changing expendable bathythermograph fall rates and their impact on estimates of thermosteric sea level rise. J. Climate 21:5657–5672.